Reprinted from Soil and Crop Sciences Society of Florida, Proceedings, Volume 61, June 10-12, 2001

Soil and Water Section

Effects of Emitter Distribution Patterns and Soil Type on Water and Solute Distribution Following Microirrigation

A. Fares, L. R. Parsons, J. Šimůnek, M. Th. van Genuchten, and T. A. Wheaton

ABSTRACT

While some furrow/flood irrigation is still used, microirrigation has already become the dominant means of supplying water to citrus groves on Florida sandy soils. Unfortunately, many microirrigation systems apply water in a non-uniform pattern. Uniformity is very important for proper irrigation, especially on sandy soils where horizontal redistribution of water is generally limited. Knowing that microirrigation systems are used to deliver fertilizers and pesticides, non-uniform water application will result in poor irrigation efficiency, fertilization, and pest control, also potential environmental contamination. The main objective of this study was to numerically study the impact of non-uniform water application on water flow and solute movement within soil profiles of ridge and flatwood soil types. Two soil profiles, typical for the Candler (hyperthermic, uncoated, Typic Quartzipsamments) and Immokalee (sandy, siliceous, hyperthermic Alfic Arenic Alaquots) soils, were used in these simulations. Results indicated 25% more water drainage under the Immokalee than under the Candler soil type. However, solute leaching was 2.5 greater under the Candler than under the Immokalee soil. These results show a strong effect of non-uniform irrigation water application on water flow and, more importantly, on solute transport, especially under ridge soil conditions. Further research will focus on the impact of water table height and water table fluctuation on water flow and solute transport processes in these two soil types.

INTRODUCTION

The use of microirrigation is rapidly increasing around the world, and is expected to remain a viable irrigation method for agricultural production in the foreseeable future. With increasing demands on limited water resources and the need to minimize adverse environmental consequences of irrigation, microirrigation technology will undoubtably play an even more important role in the future. Growers and other microirrigation users are continually seeking new applications, such as waste water reuse, that will continue to provide new challenges for designers and irrigation managers.

Microirrigation is a system that operates under low pressure (100-200 KPa) with small-sized wetting patterns and low discharges. Microirrigation systems can apply water and fertilizer directly to individual plants or trees and reduce the wetted area by wetting only a fraction of the soil surface. Thus, water is applied directly to the root zone. Some microirrigation systems are capable of wetting only a fraction of the root zone while supplying adequate water to satisfy crop water requirements.

Spray or spinner emitters are often preferred over drip systems for orchards since they provide a larger-diameter wetting pattern. This characteristic is especially desirable in areas with coarse-textured soils (e.g., Florida sandy soils), where lateral soil water movement is limited (Boman, 1989). Non-uniform surface water application on sandy soils often results in uneven movement of the moisture front through the soil profile, with part of the rootzone showing excess water losses while another part may receive little or no irrigation water. Since microirrigation systems are often used to deliver fertilizers and pesticides, this non-uniform water application will result in poor irrigation, fertilization, and pest control, and can potentially lead to environmental contamination.

Non-uniformity of water application by microirrigation systems has several causes. Some sources of poor irrigation uniformity are topographical (slope) variations, hydraulic friction losses in pipes and fittings, poor quality inherent in emitter design and manufacture, multiple emitters of different specifications within a single block, nozzle wear, and deposits in orifices from poor filtration or water quality. Most manufacturers supply a specification sheet detailing their sprinkler designs that includes a wetting pattern measured when the sprinklers are operating at a stated pressure. The distribution characteristic of a given microirrigation system is defined as the ratio (in percentage) of the area that receives more than half the average application to the total wetted area (Merriam and Keller, 1978).

Boman (1989) evaluated several microsprinkler spinner and spray emitters to determine their distribution and uniformity patterns. He found that the spinner types of emitters had higher uniformity of water application than spray types under no-wind conditions. In fact, most of the tested spray emitters showed 50 to 75% of the wetted area received insignificant water application while 10 to 15% of the wetted area received more than three times the average application. Our extensive literature review revealed little or no work on the implication of non-uniform surface water applications on water movement and solute transport within the soil profile.

The main objective of the current work is to use a numerical model, HYDRUS-2D, to study the impact of the emitter patterns on water flow and solute transport in two different soil types.

A. Fares, Nat. Res. and Environ. Manage. Dep. Univ. Hawaii, 1910 East-West Rd., Honolulu, HI 96822; L. R. Parsons and T. A. Wheaton Univ. of Florida, Cit. Res. and Educ. Center, 700 Experiment Station Rd., Lake Alfred, FL 33850; J. Šimůnek and M. Th. van Genuchten, U.S. Salinity Laboratory, USDA, ARS 450 Big Springs Rd., Riverside, CA 92507-4617. Contribution of the Citrus Res. and Educ. Center. This research was supported by the Florida Agric. Exp. Stn. and is approved for publication as Journal Series No. R-08475.
*Corresponding author (AFares@Hawaii.edu).
Contribution published in
Soil Crop Sci. Soc. Florida Proc. 61:46-56 (2002).

MATERIALS AND METHODS

HYDRUS-2D

In this study we used a software package, HYDRUS-2D, a computer program developed to simulate the two-dimensional movement of water, heat, and multiple solutes in variably saturated media (Šimůnek et al., 1999). The software package consists of the HYDRUS2 computer program and the interactive graphics-based user interface HYDRUS-2D. The HYDRUS2 program numerically solves the Richards' equation for variably-saturated water flow and convection-dispersion equations for heat and solute transport. The flow equation incorporates a sink term to account for water uptake by roots. The solute transport equation considers transport due to dispersion and convection with flowing water. The governing flow and transport equations are solved numerically using Galerkin-type linear finite element schemes.

HYDRUS2 can handle flow regions delineated by irregular boundaries. The flow region itself may be composed of nonuniform soils with different soil physical characteristics. Soil hydraulic parameters can be represented analytically using different hydraulic models such as the van Genuchten (1980) and Brooks and Corey (1964) equations. HYDRUS2 incorporates hysteresis in the soil-water retention function by using the empirical model introduced by Scott et al. (1983).

The MS Windows-based Graphics User Interface manages the geographical, hydrogeologic and physical inputs required to run HYDRUS2, as well as grid design and editing, parameter allocation, problem execution, and visualization of results. Simulated areas of interest can be zoomed into, and the vertical scale can be enlarged for cross-sectional views. Output graphics include 2D contours (isolines or color spectra) in aerial or cross-sectional view for pressure heads, water contents, velocities, and concentrations. It is also possible to obtain velocity vector plots, animation of graphic displays for sequential time steps, line-graphs for selected boundary or internal sections, and for variable-versus-time plots. HYDRUS2 was validated under different field and laboratory conditions (Šimůnek and Genuchten, 1999; Vrugt et al., 2001). Several typical applications can be found at http://www.ussl.ars.usda.gov/models/hydrus2d.htm.

Simulations

A two-dimensional soil transect, 1-m wide and 1.5-m deep, was used in this study. To simulate non-uniform irrigation, the upper boundary of the simulated profile was divided into four equal segments, each 0.25-m wide. According to Boman (1989), part of the wetted area under spray emitters can receive more than three times the average application, while the remaining surface may receive insignificant water. Based on this observation, the four upper soil segments were divided into two high and two low water input areas where the former one received four times as much water (4 cm h^{-1}) as the latter (1 cm d^{-1}) (Fig. 1). A constant potential evapotranspiration rate ET_0 (0.1 cm h^{-1}) was imposed on the upper boundary regardless of the water input rate. These high water input and ET_0 rates were used to magnify their effects over a short period of time. Free drainage (i.e., gravity flow) and boundary conditions were used at the bottom and sides of the soil profile, respectively. A tracer of 30 mmol cm^{-3} concentration was assumed to be applied with the incoming water during the first hour of simulation. After the first application, irrigation water was solute-free. Simulations were run for 36 h with hourly alternating irrigation and continuous evapotranspiration.

Two Florida soils typical for the citrus growing region were used in the simulations: a Candler fine sand and an Immokalee soil. The Immokalee soil profile consists of deep or very deep, poorly drained or very poorly drained soils that were formed from sandy marine sediments. A Spodic horizon (B_h) usually exists 0.9 m below the soil surface. This soil type can often be found on flatwoods and in depressions of the peninsular Florida. The Immokalee profile, which has a fluctuating water table is a typical soil of southwest Florida. The Candler soil profile consists of very deep, excessively drained, rapidly permeable soils formed on thick beds of eolian or marine deposits of coarse-textured materials. The Candler soils occur in the central Florida ridge area. Selected physical properties of different horizons of the Candler fine sand and the Immokalee soil, as reported by Sodek et al. (1990), are given in Table 1.

For the following simulations, we assumed a homogeneous soil profile for the Candler fine sand with a single set of hydraulic properties, i.e., the soil water release (retention) curve and the hydraulic conductivity-soil water suction relationship. The soil profile for the Immokalee soil was assumed to consist of two distinct soil horizons. The top 1 m had physical properties similar to the Candler soil, while the lower 0.5 m portion of the profile was assumed to have the B_h properties (Fig. 1).

Florida Ridge citrus irrigated with under-tree microsprinklers generally has a shallow root system with over 70% of the roots in the top 60 cm (Fares and Alva, 2000). Seventy five percent of the root system was assumed to be located in the top 1 m of the soil profile and the remaining 25% in the lower 0.5 m. An initial condition of 100-cm water matric suction was assumed throughout the entire simulated system. Using the soil water release curves (Fig. 1), such initial conditions resulted in more water being stored in the lower Immokalee horizon (<0.5 m) than in that of the Candler soil.

HYDRUS-2D allows users to specify the location of one or more monitoring points within the simulated profile. The model then monitors the amount of water and solute that moves across these points and establishes breakthrough curves at these locations. We specified six monitoring points through the simulated profile as shown in Fig. 2.

RESULTS AND DISCUSSION

Calculated water contents in the simulated soil profile at 3, 9, 25, and 30 h are shown in Fig. 3. In both soil types, higher water contents under high water input areas and during water input periods translated into differ-

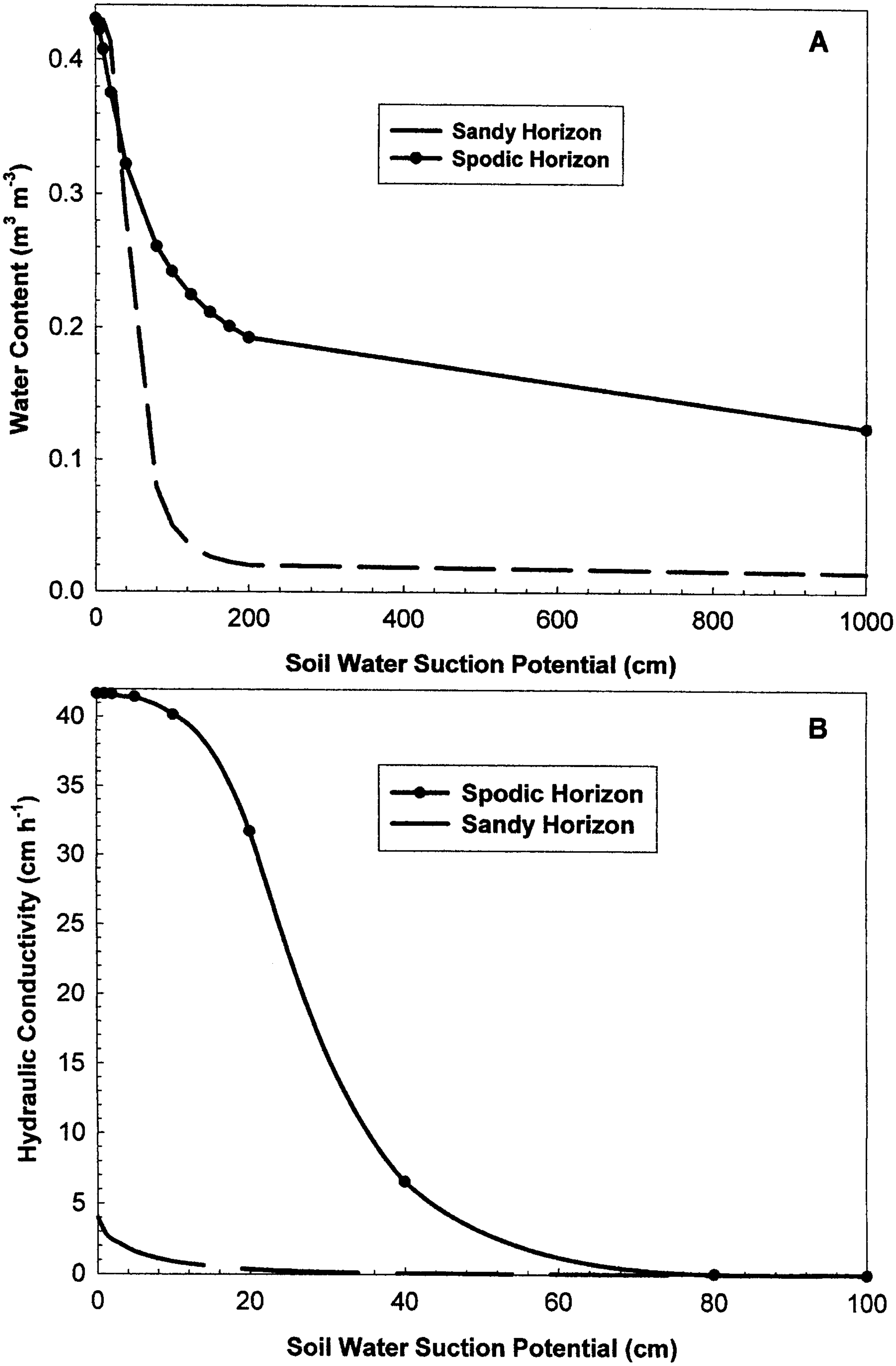

Fig. 1. The soil water release curves (A) and the hydraulic conductivity functions (B) as function of the soil water suction for the sandy and Spodic horizon for the Candler and Immokalee soils.

Table 1. Selected physical properties of a Candler fine sand sampled at various depths.

Soil depth	Bulk density	Horizon	Particle size distribution: Sand	Silt	Clay	Sat. hydraul. conduc.	Texture class	Soil moisture content: 1/100 M Pa	1/30 M Pa	1.5 M Pa
cm	g cm^{-3}		g kg^{-1}			m d^{-1}		cm^3 cm^{-3}		
0-20	1.59	Ap	973	9	18	5.21	FS	0.10	0.07	0.02
20-48	1.52	E_1	974	12	14	9.48	FS	0.06	0.04	0.01
48-94	1.51	E_2	978	8	14	8.52	FS	0.03	0.03	0.01
94-132	1.61	E_3	976	15	9	7.27	FS	0.05	0.3	0.01
132-245	1.55	E/Bk	977	14	9	6.96	FS	0.04	0.02	0.01
245-275	1.55	Btg	544	49	407	0.24	SCL	0.33	0.31	0.23

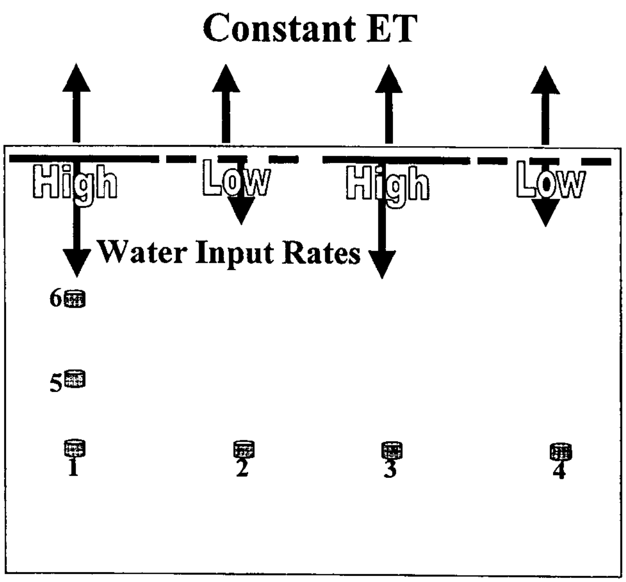

Fig. 2. Schematic of simulated profiles that shows the locations of water input, evapotranspiration (ET), and the the six observation points (OP1-OP2).

ent flow velocities (not shown here) throughout the lower part of the simulated system. There was almost no difference between the two soil profiles 9 h after the start of the simulation, with most water moving downward. However, as the wetting front reached the interface between the sandy and Spodic horizons of the Immokalee soil, some water also moved laterally. Water contents of the top 1m at 25 h after the start of the simulation seem to be similar to those at 3 and 9 h. Lateral water redistribution in sandy soils is generally limited (Boman, 1989). A dry pocket can be seen just above the spodic horizon, on the right side of the system, 9 h after the start of the simulation. Toward the end of the simulation, i.e., at 30 h, the soil water content in the Candler soil profile was more homogeneous than that of the Immokalee profile. The main reason for this difference is the presence of the Spodic horizon in the Immokalee soil that has different hydraulic properties (Fig. 1, Tables 1 and 2).

Snapshots of the solute concentration in the soil profiles at 3, 16, 22, and 26 h are shown in Fig. 4. As expected, the distributions in the two soils were essentially the same during the first 3 h since all input parameters were the same for the top horizon. The simulated solute was a non-reactive tracer, and thus its concentration distribution in the soil profile at different times resembles that of the water front with which it is moving, except for some separation of the water and solute fronts because of solute mixing with the initial water. Beyond 1-m depth, spreading of the solute front is more pronounced in the Candler soil than in the Immokalee soil due to the higher hydraulic conductivity of the former soil. There is almost 1 m difference between the deepest and shallowest parts of the solute front after 25 h of simulation for the Candler soil type. This uneven spreading of the solute through the soil profile was slowed substantially in the Immokalee soil by the Spodic horizon. After 26 h of the start of the simulation, most of the solute was flushed out of the Candler soil profile, most of the solute remained within the Immokalee soil profile (Fig. 5B).

Drainage fluxes out of the two simulated systems were negligible during the first 13 and 22 h of the simulation for the Candler and Immokalee soils, respectively (Fig. 5A). Based on the cumulative drainage out of the Candler soil (Fig. 5A), hourly average drainage fluxes were 1.4 and 2.1 cm h^{-1} during the two distinct periods (13-26 h) and (27-36 h), respectively.

Table 2. Selected physical properties of a Immokalee soil sampled at various depths.

Soil depth	Bulk density	Horizon	Particle size distribution: Sand	Silt	Clay	Sat. hydraul. conduc.	Texture class	Soil moisture content: 1/100 M Pa	1/30 M Pa	1.5 M Pa
cm	g cm^{-3}		g kg^{-1}			m d^{-1}		cm^3 cm^{-3}		
0-18	1.35	A	979	17	4	8.40	S	0.08	0.06	0.02
18-46	1.58	E_1	988	5	7	12.30	S	0.04	0.03	0.01
46-99	1.62	E_2	984	10	6	10.20	S	0.04	0.03	0.01
99-147	1.35	B_h	941	45	14	0.90	S	15.70	11.80	0.03
>147	1.57	E	973	20	7	2.60	S	5.5	3.0	0.00

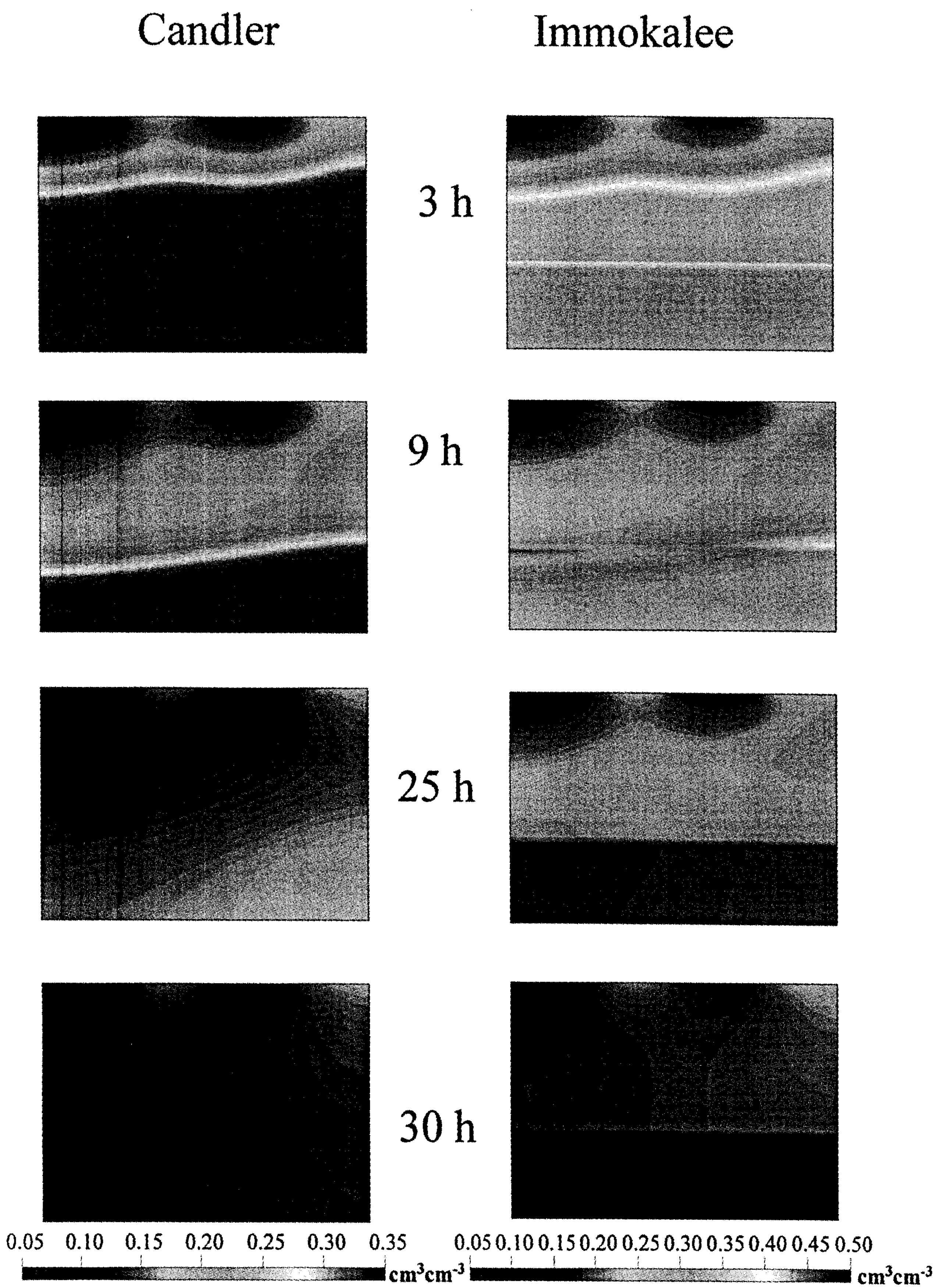

Fig. 3. Water content distributions in the simulated soil profiles at 3, 9, 25, and 30 h after the start of the simulation for the Candler and Immokalee soils (not to scale).

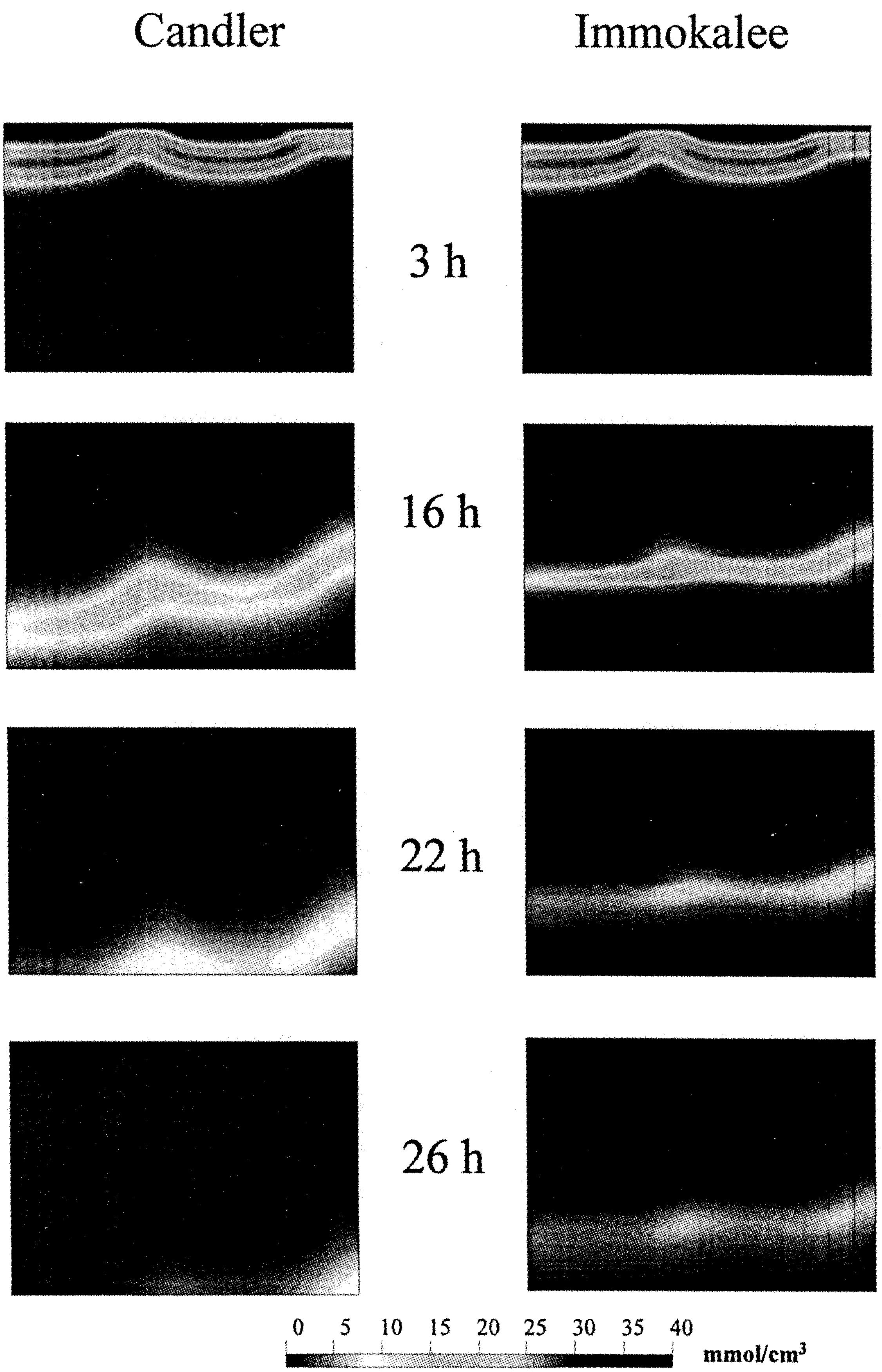

Fig. 4. Solute concentrations in the simulated soil profiles at 3, 16, 22, and 26 h after the start of the simulation for Candler and Immokalee soils (not to scale).

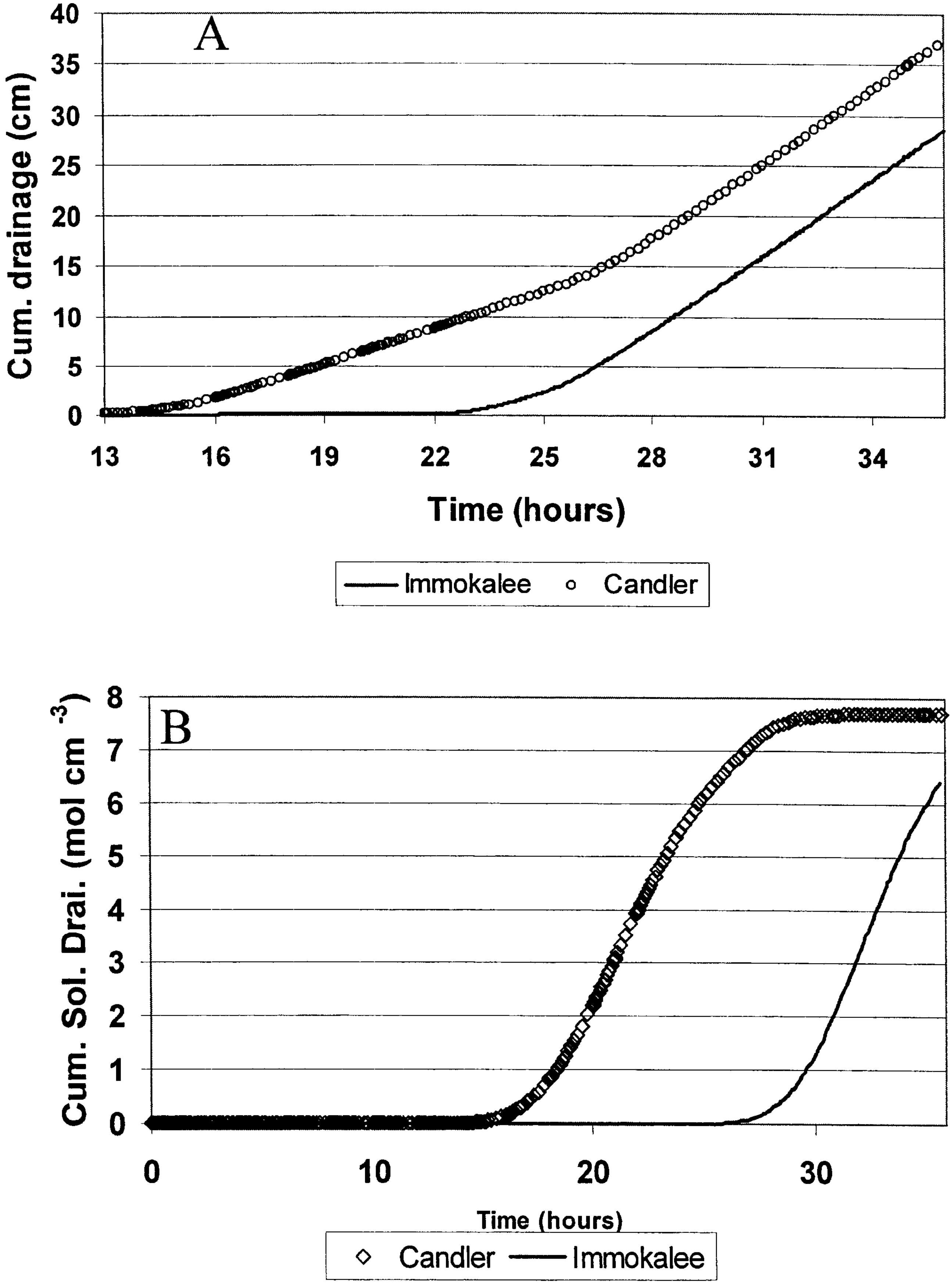

Fig. 5. Cumulative simulated water losses (A) and solute leaching (B) at the lower boundary of the simulated system for the Candler and the Immokalee soils.

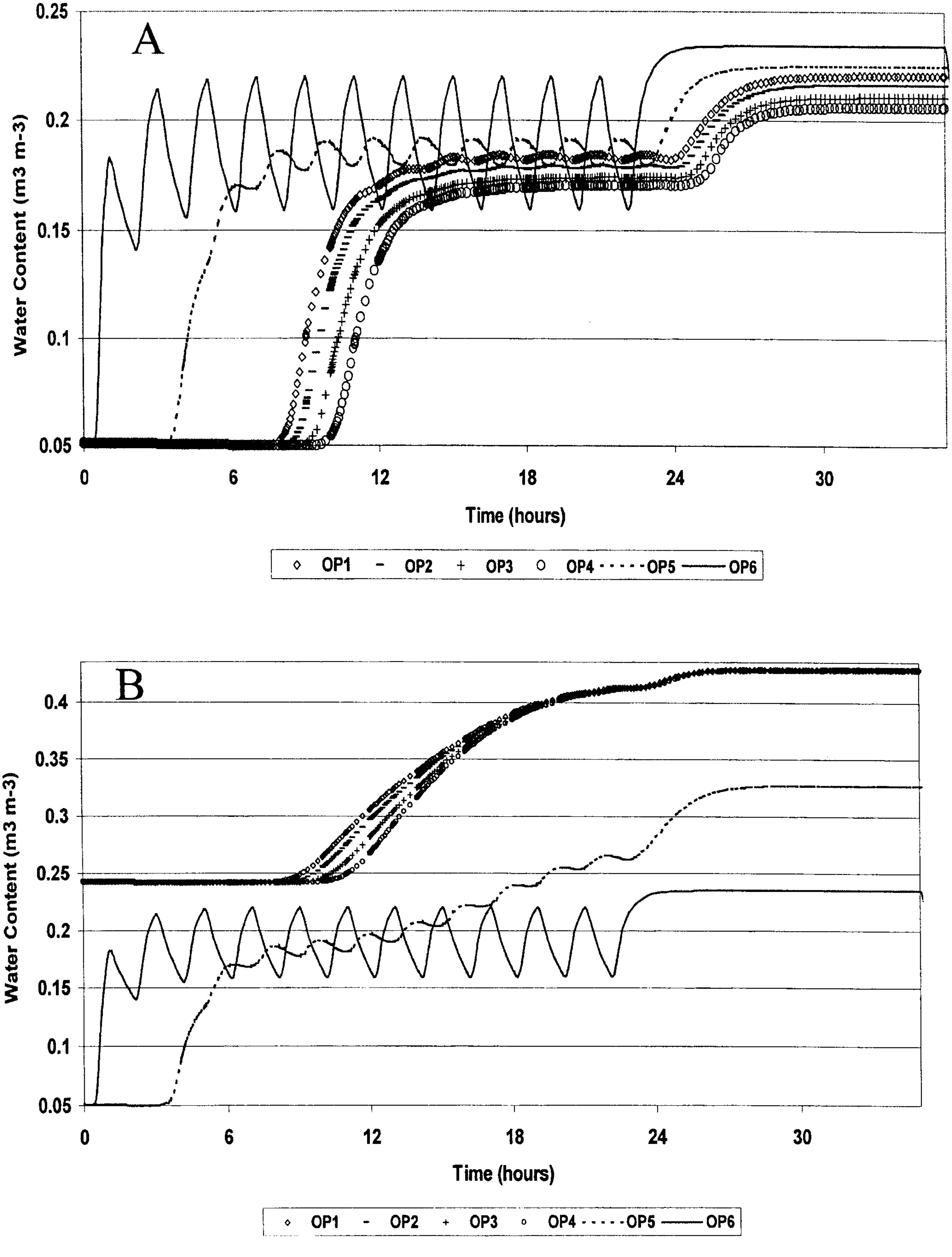

Fig. 6. Water breakthrough curves at the six observation points chosen through the simulated soil profile for the Candler (A) and Immokalee (B) soils.

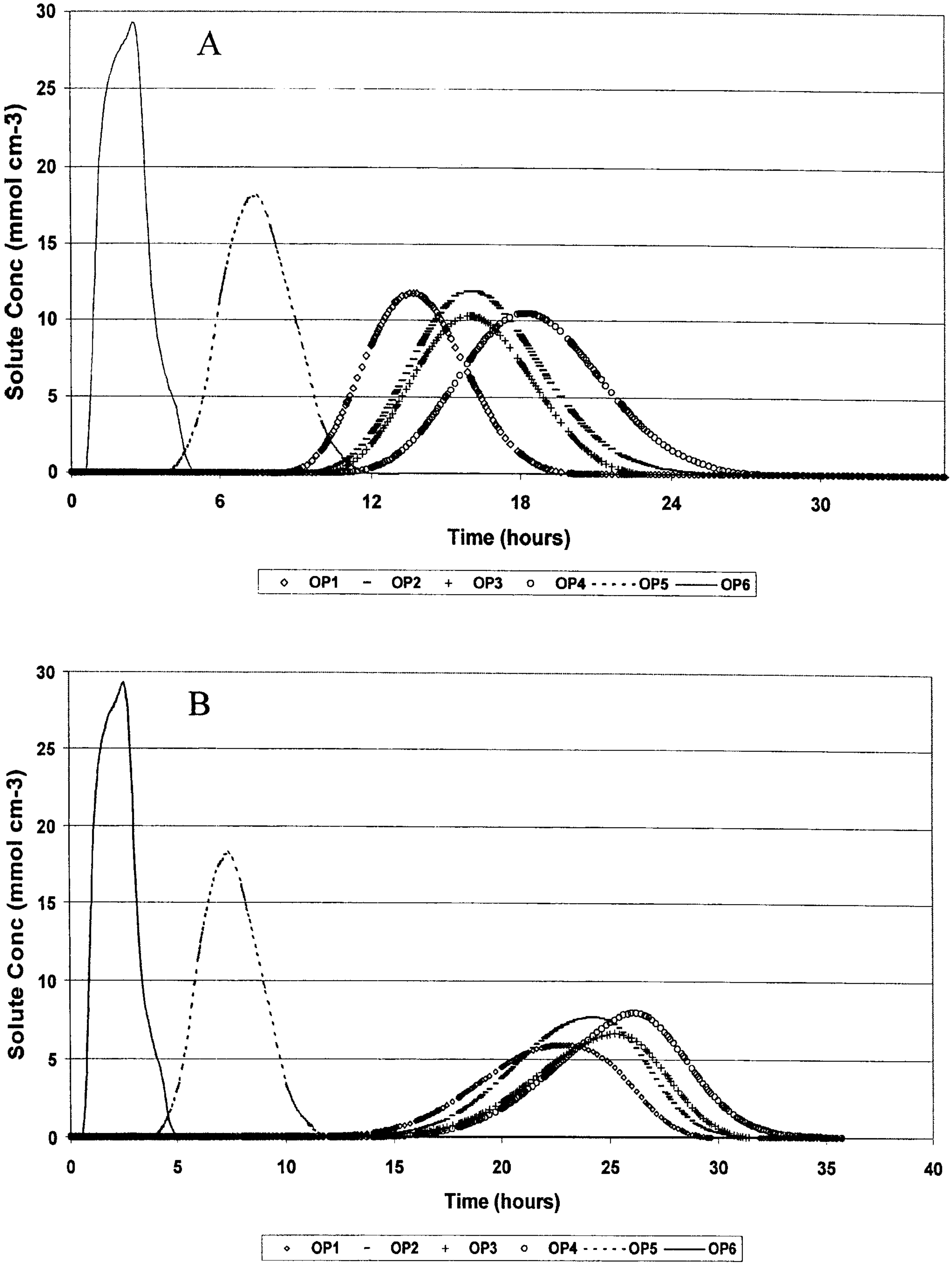

Fig. 7. Solute breakthrough curves at the six observation points chosen through the simulated soil profile for the Candler (A) and Immokalee (B) soils.

The water contents and solute-breakthrough curves at the six monitoring points of both simulated soil profiles are presented in Fig. 6A, B and Fig. 7A, B, respectively. Initial conditions in terms of the pressure head for both soil types were the same, with a constant value of -100 cm applied throughout the entire soil profile. This initial matric potential resulted in different initial water contents in both soil types as a result of differences in the retention curves of the Spodic and sandy layers. According to the soil water release curves (Fig. 1), the Spodic horizon has higher water content than the sandy horizon at the same matric potential. At this matric potential, the spodic horizon in the lower 0.5 m of the Immokalee soil profile was wetter than that of the Candler soil during the simulation time.

Regardless of the soil type, the water content in the top two observation points (OP5 and OP6) showed similar behavior. This is expected since the top 1 m of the two simulated systems is the same. However, there was a very distinct behavior of the water content in the other four observation points (OP1-OP4) between the two soil types. Because the water front tended to move horizontally in fine texture soil types, such as the Spodic horizon, the water content of the first four observation points of the Immokalee soil did not show any obvious difference except during the first period of the water front movement (8-12 h). This was not the case for the same observation points of the Candler soil. For this soil type, every observation point had a different water content behavior and was distinct from the rest.

The solute breakthrough curves at the six monitoring points varied considerably as a result of their vertical and horizontal positions and as a function of soil type (Fig. 7A, B). Because of their shallow vertical positions, OP5 and OP6 received and flashed out the solute before the solute reached the other observation points of the two soil types. The maximum solute concentration of the observation points is closely related to the vertical positions (Fig. 7A). As the pulse of solute moves down the soil profile, it is diluted by the following solute free water front. The extended horizontal spread of the water front and consequently the solute pulse in the spodic horizon resulted in a decrease of the solute concentration at each of the low four observation points of the Immokalee soil as compared to those of the Candler soil. For the Immokalee soil, significant solute leaching started 27 h after the start of simulation, 9 h later than for the Candler soil. Regardless of the soil type, the water and solute front movements are similar for the first few hours before they reach the Spodic horizon in the Immokalee soil. By comparison, there is less separation between the wetting and concentration fronts in the lower part of the much drier Candler soil.

At the end of the simulation, there was 23% more water drainage from the Candler soil than from the Immokalee soil (Fig. 5A). The excess drainage for the Candler soil resulted in 35% more solute losses from the Candler soil than from Immokalee. This difference is due to the difference in hydraulic properties (hydraulic conductivity) of the lower horizons of the two soils. The residence time of the solute in the lower 0.5m of the Immokalee soil simulated profile (Spodic horizon) is higher than that in the Candler soil because of the pronounced horizontal spread of the water front in the Spodic horizon of the former soil type. Thus, there were 35% more solute losses from the Candler soil than from the Immokalee soil by the end of the simulation.

SUMMARY AND CONCLUSIONS

HYDRUS2D, a numerical model for simulating two-dimensional movement of water, solute and heat was used to evaluate effects of irrigation rate spatial variability due to emitter patterns on water flow and solute transport under two different soil types. Simulation results showed that emitter patterns resulted in uneven movement of the water front through the soil profile. This process has important implications for irrigation scheduling and fertilizer application. During irrigation scheduling, irrigators assume uniform water front movement through the soil profile and base their calculations on this assumption. Our current work shows significant differences of the water front and solute movement in the top sandy soil profile and the lower Spodic horizon. Water and solute tend to move vertically in the sandy profile and more horizontally in the Spodic horizon. Under these short term simulation conditions, the Candler soil seems to be more susceptible to the effect of uneven irrigation application by emitters than the Immokalee soil. Our results suggests that non-uniform water applications will produce more heterogeneous solute leaching patterns in coarse-textures soil profiles having relatively low initial water contents, as compared to fine-textured soils having higher initial (and usually final) water contents. Also, for given application rates, the soil water retention (release) curve is more important than the saturated and unsaturated hydraulic conductivity of the soil profile in defining the leaching pattern. Further work is needed to study the behavior of different solutes such as reactive solutes with degradation and volatilization for long and short term simulations. Field work is also needed to validate results of these simulations.

REFERENCES

Boman, B. J. 1989. Distribution patterns of microirrigation spinner and spray emitters. Applied Eng. Agric. 5:50-56.

Brooks, R. H., and A. T. Corey. 1964. Hydraulic properties of porous media. Hydrology Pap. No. 3. Colorado State Univ., Ft. Collins.

Fares, A., and A. K. Alva. 2000. Evaluation of capacitance probes for optimal irrigation of citrus through soil moisture monitoring in an entisol profile. Irrig. Sci. 19:57-64.

Merriam, J. L., and J. Keller. 1978. Farm irrigation system evaluation: A guide for management. Utah State Univ., Logan.

Scott, P. S., G. J. Farquhar, and N. Kouwen. 1983. Hysteresis effects on net infiltration, p. 163-170. *In* Advances in Infiltration, Pub. 11-83, Am. Soc. Agri. Eng., St. Joseph, MI.

Šimůnek, J., and M. Th. van Genuchten. 1999. Using the HYDRUS-1D and HYDRUS-2D codes for estimating unsaturated soil hydraulic and solute transport parameters. p. 1523-1536. *In* van Genuchten et al. (ed.). Characterization and measurement of the hydraulic properties of unsaturated porous media, Univ. of California, Riverside.

Šimůnek, J., M. Šejna, and M. Th. van Genuchten. 1999. The HYDRUS-2D software package for simulating two-dimensional movement of water, heat, and multiple solutes in variable saturated media. Version 2.0, IGWMC-TPS-53, International Ground Water Modeling Center, Colorado School of Mines, Golden.

Sodek, F., III, V. W. Carlisle, M. E. Collins, L. C. Hammond, and W. G. Harris. 1990. Characterization data for selected Florida soils. Soil Sci. Rep. No. 90-1. Univ. of Florida, Gainesville.

van Genuchten, M. Th. 1980. A closed-form equation for predicting the hydraulic conductivity of unsaturated soil. Soil Sci. Soc. Am. J. 44:892-898.

Vrugt, J. A., J. W. Hopmans, and J. Šimůnek. 2001. Calibration of a two-dimensional root water uptake model for a sprinkler-irrigated almond tree. Soil Sci. Soc. Am. J. 65:1027-1037.